ORIGINAL PAPER

First application of benzotriazole as a dye additive to dye-sensitized solar cells: electrochemical device characterization

Gideã Taques Tractz[1] · Ana Paula Camargo Matheus[2] · Leticia Fernanda Gonçalves Larsson[2] · Paulo Rogério Pinto Rodrigues[2]

Abstract

Dye-sensitized solar cell, known as an emergent technology, has been attracted attention around the world. It has been easily produced by a mesoporous semiconductor oxide (SO), with a dye. On the other hand, some unexpected reactions as the back-electron recombination, reducing the solar cell efficiency. The presence of some molecules to act as an oxide passivation might rise up the collection reaction rate, and enhance the photoelectrochemical solar system parameters. The molecule used as a dye additive, must effortlessly adsorb in SO and potentiate the dye deaggregation. This work aims to study the benzotriazole (BTAH) insertion in DSSC with TiO_2, evaluating its capability as a passivator molecule in such PV technology. The electrochemical results showed better electrochemical energy conversion efficiency with lower resistance with BTAH at 2.0 mg mL^{-1}, achieving a $j_{sc} = 9.92 \pm 0.26$, $V_{oc} = 0.770 \pm 0.022$, FF $= 0.557 \pm 0.014$, $\eta = 4.26 \pm 0.13$ with superior electron lifetime and amazing recombination prevention.

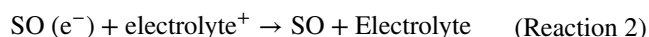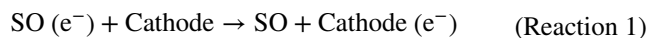**Keywords** PV system · BTAH · IMPS · IMVS · DSSC

Introduction

The use of semiconductor oxides with solar incidence is a promising technology to energy conversion [1–3]. Recent application of chenodeoxycholic acid-substituted dyes, in the third generation of dye-sensitized solar cells (DSSCs) raised up a new study area in PV systems [4]. The capability of suppressing dye-dye interactions and anchoring in the oxide surface become an excellent alternative in DSSCs development.

Dye-sensitized solar cells are made by the use of an electron transport material on transparent conductor oxide (TCO), acting as a scaffold material. There is also the presence of a dye, a photosensitive molecule that inject electron by solar irradiation, providing a charge flow responsible for the solar energy conversion [1–3].

Simply, the solar cell operating is based on the dye ability to inject electrons in the conduction band of scaffold oxide, usually TiO_2 [5], ZnO [6], and SnO_2 [7] with solar energy incidence. The injected electrons, moves through a TCO to a cathode catalyst, generating a charge flow as demonstrated in Reaction 1, (where SO is the semiconductor oxide).

$$SO\ (e^-) + Cathode \rightarrow SO + Cathode\ (e^-) \quad \text{(Reaction 1)}$$

$$SO\ (e^-) + electrolyte^+ \rightarrow SO + Electrolyte \quad \text{(Reaction 2)}$$

The intermediation of redox species is provided by an electrolyte that has been able to capture the electron in the cathode, reducing the dye [8, 9]. However, another reaction has been able to occur in the oxide/dye/electrolyte interface, the back-electron recombination (Reaction 2) [5, 10].

Suppressing the oxide-electrolyte recombination is one of the most studied ways to produce DSSC with improved photoelectrochemical parameters [11]. From this standpoint, many technologies have been used to reduce Reaction 2: push–pull dyes [12], using mix oxides [13, 14], and electrolyte additives [15]. Recently, Rodrigues and co-workers, [11]

✉ Gideã Taques Tractz
  gideatractz@utfpr.edu.br

1 Chemistry Departament, Universidade Tecnológica Federal do Paraná, Campo Mourão, Campo Mourão, PR 85040-080, Brazil

2 Chemistry Departament, Universidade Estadual do Centro Oeste, Campus CEDETEG, Guarapuava, PR 85040-080, Brazil

applied the poly (4-vinyl pyridine), observing a TiO$_2$ surface passivation, able to suppress the back-electron recombination and increasing the current, even at low dye loading [16, 17]. This related study shows that is possible to use organic additives in dye solar cells, such as benzotriazole (BTAH).

Benzotriazole is used as an effective inhibitor for several metal alloys and demonstrates high solubility in many aqueous media, good thermal stability, and has been able to chemical adsorbed in metal surface, due to nitrogen presence. In other words, some impressive advantages over the use of chenodeoxycholic acid. Furthermore, the equilibrium involving BTAH$^-$ and BTAH^{2-} can contribute to physisorption and modulation of a space charge layer in a semiconductor/electrolyte interface [15, 16].

With a dye, BTAH might act efficiently avoiding dye aggregation, and shifting the oxide fermi level (E_f), influencing the charge separation and photoelectrochemical values of the cells [15, 17, 18]. Regarding toxicity and recent applications, concentrations lower than 2.10^{-2} mol L^{-1} are not toxic and relate to its use, beyond the corrosion inhibitor, BTAH has been used as protease inhibitor to several virus classes, such as Corona Virus (SARS-CoV) [19, 20].

This work aims to first report the application of BTAH as an additive to DSSC and understand their role in photoanode/electrolyte interface, as a new alternative to produce systems with superior photoelectrochemical parameters.

Experimental

The oxide paste was produced with 3 g the TiO$_2$ (*Aldrich*® 25 nm 100% anatase), 1 ml of polyethylene glycol, 0.1 mL of acetylacetone, 4 mL of deionized water, and 0.1 mL of Triton-X. TiO$_2$ suspension was coated by Doctor Blading method under FTO (~ 7 Ω sq^{-1} *Aldrich*®). After deposition, the films were sintered at 450 °C for 30 min followed by immersion for 12 h in N719 commercial dye solution (2.5×10^{-4} mol L in ethanol) containing 0.148 mg mL^{-1}; 2 mg mL^{-1} and 20 mg mL^{-1} of BTAH [10].

The electrolyte was fabricated by mixing 0.5 mol L^{-1} tert-butylpiridine, 0.6 mol L^{-1} tetrabutylammonium, 0.1 mol L^{-1} lithium iodide, and 0.1 mol L^{-1} of resublimate iodine, in methoxypropionitrile [5]. The cathode catalyst was produced by Pt electrodeposition under FTO, using a three-electrode system, with FTO as a working electrode, Pt as a counter electrode, and Ag/AgCl as a reference electrode, using K$_2$PtCl$_6$ dissolved in HCl as electrolyte [18].

The solar cells were assembled in sandwich format, in an active area of 0.2 cm^2. The electrochemical measurements of *j-V* curves were taken in Zhenium Zahner@ potentiostat with a solar simulator provided by a Xenon lamp at 100 mW cm^{-2}. Electrochemical Impedance Spectroscopy (10 mHz–10 kHz at 10 mV of perturbation),
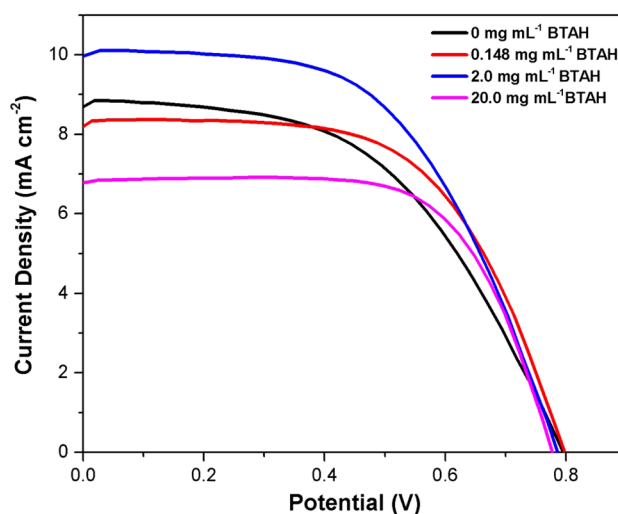

Fig. 1. *j-V* curves to solar cells with different BTAH amounts

Table 1. Photoelectrochemical parameters to solar cells with different BTAH amounts

BTAH (mg mL^{-1})	j_{sc} (mA cm^{-2})	V_{oc} (V)	FF	η (%)
0	8.52 ± 0.48	0.802 ± 0.009	0.555 ± 0.068	3.78 ± 0.09
0.148	8.09 ± 0.38	0.780 ± 0.004	0.592 ± 0.003	3.74 ± 0.01
2.0	9.92 ± 0.26	0.770 ± 0.002	0.557 ± 0.014	4.26 ± 0.03
20.0	6.21 ± 0.89	0.767 ± 0.005	0.628 ± 0.045	3.01 ± 0.06

Intensity Modulated Photovoltage Spectroscopy (IMVS), and Intensity Modulated Photocurrent Spectroscopy (IMPS) (100 mHz–1 kHz at 10 mW of perturbation) were performed in an auto lab potentiostat from Metrohm®, coupled with a led lamp of 530 nm at 50 mW cm^{-2}.

Results and discussion

In Fig. 1 it is depicted the j-V curves to dye solar cells analyzed, and the photoelectrochemical results in Table 1.

It is well observed a reduced open circuit potential (V_{oc}) to the cells with the BTAH amounts. It can be explained by the reduction of TiO$_2$ conduction band edge, due to the protonation of oxide by *N* group contained in BTAH molecules [19, 20]. The reduced V_{oc} can be seen as a negative point to solar cell working, by potentiated charge recombination reaction [21]. On the other hand, some papers demonstrated no relation between lower V$_{oc}$ with back-electron recombination suppression, as showed by Guimaraes and co-workers [12].

As the V_{oc} is the difference between the quasi-Fermi level and the standard redox potential to the electrolyte, it is noted

that BTAH amount in N719 dye has been able to shift the E_f level to more positive potentials [22]. One possible key to improve V_{oc} values is synthesizing new dyes containing BTAH in their own composition, not acting only as a spacer, even to composing the sensitizing material [4].

The photoconversion energy efficiency (η) was obtained using Eq. 1, where j_{sc} is the short circuit current, FF fill factor, and P_{in} the incident power [23].

$$\eta = \frac{j_{sc} V_{oc} FF}{P_{in}} x100 \tag{1}$$

It has been observed superior η value (4.26 ± 0.03) to the cell prepared with BTAH in 2.0 mg mL^{-1} condition when compared to the standard cell (3.78 ± 0.09). It demonstrated an efficiency boost of 12.8% in the energy conversion, due to superior photocurrent to the same BTAH condition. The η values, when compared to literature were reduced since it was not made TiCl$_4$ treatment and the scattering TiO$_2$ layer was not used [24].

It is also observed, that BTAH in the concentration of 0.148 mg mL^{-1} has not demonstrated a different behavior when compared to bare cells (due to deviation values). In higher concentrations of 20.0 mg mL^{-1} and superior, it is expected an inhibition process of the charge collection, because BTAH molecules must occupy all the TiO$_2$ active layer, reducing the current and PCE values [25]. The space charge region in TiO$_2$/electrolyte interface (SCR) should be undergoing changes, improving electron collection rate (Reaction 1), and reducing the recombination reaction demonstrated by Reaction 2 [26]. For a better analysis of its supposed behavior, EIS measurements were taken and Bode diagram is depicted in Fig. 2.

In Bode diagram of Fig. 2, it is observed two different regions. Higher frequencies are related to Pt/Electrolyte interface and in lower frequencies, SCR interface [12]. It is noted a shift to reduced frequency values to the region of working electrode. As frequency and time are inversely proportional, lower frequencies mean a slowness in the charge transfer process, and to confirm this resistance, Nyquist plots (Fig. 3) were fitted using a simplified equivalent circuit (Fig. 1.SI) [11, 27–29]. The resistance values of TiO$_2$/Dye, BTAH interface (R_{WE}), and Pt/Electrolyte with the chemical capacitance (C_μ) were estimated in Table 2.

By adding BTAH in 2.0 mg mL^{-1} concentration, it is noted a great minimization of charge transfer resistance in TiO$_2$/dye, BTAH/electrolyte interface. This behavior demonstrates a more conductive and less resistive system which should facilitate the charge transport mechanism, being a great advantage when compared to similar additives applications, that showed an increase in R_{WE} [8]. At higher values of added benzotriazole, R_{WE} starts to rise up, proving that at high amounts (> 20 mg mL^{-1}) it is obtained a solar system
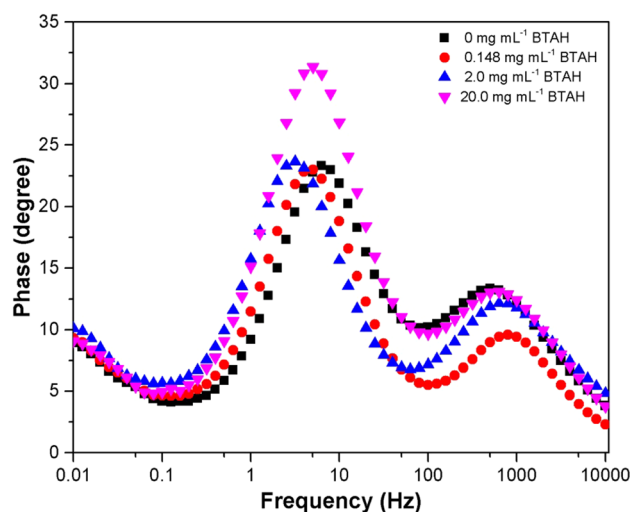

Fig. 2. EIS Bode diagram to solar cells with different BTAH amounts

with a charge process transfer minimized. Nyquist diagrams in Fig. 3 also demonstrate the same reduction in Z_i values, with BTAH addition, which corroborates the j_{sc} and η values obtained from j-V curves (Table 1).

For the chemical capacitance (C_μ), it is observed proportional decreased values with the amounts of BTAH added, as also verified in C_μ versus f curves of Fig. 2.SI. This behavior has been shown a reduce in the electrical double layer formed at working electrode interface.

With equal or higher amounts of BTAH (> 20.0 mg mL^{-1}), it is supposed to obtain an increased resistance value, due to TiO$_2$ pores filling that would be filled by the photosensitive molecule, decumulating the C_μ. It is clear that there is a concentration threshold that potentiates the solar cell photoelectrochemical parameters which must be well analyzed. A schematic overview about these discussions is shown in Fig. 4.

As shown in Fig. 4, a vacancy site, due to dye absence is an active site of recombination reaction, caused by electrolyte filling [30]. With BTAH insertion, there is a deaggregation of the dye, due to a competition for a TiO$_2$ surface site. As benzotriazole molecules present a reduced size, it is able to fill the vacancy sites, avoiding by a steric hindrance and oxide adsorption effect, the contact of TiO$_2$ and oxidized electrolyte. As demonstrated in some papers, BTAH has been able to easily adsorb in several materials [19, 20]. The charge recombination process should still occur, due to conjugated duple bonds, however with a slower speed.

As Reaction 1 and 2 occurs in TiO$_2$/electrolyte interface, it is not feasible to study the processes separately by EIS diagram. To well analyze the back-electron recombination and charge collection the IMVS and IMPS diagram were performed on cells and are depicted in Fig. 5A-B.
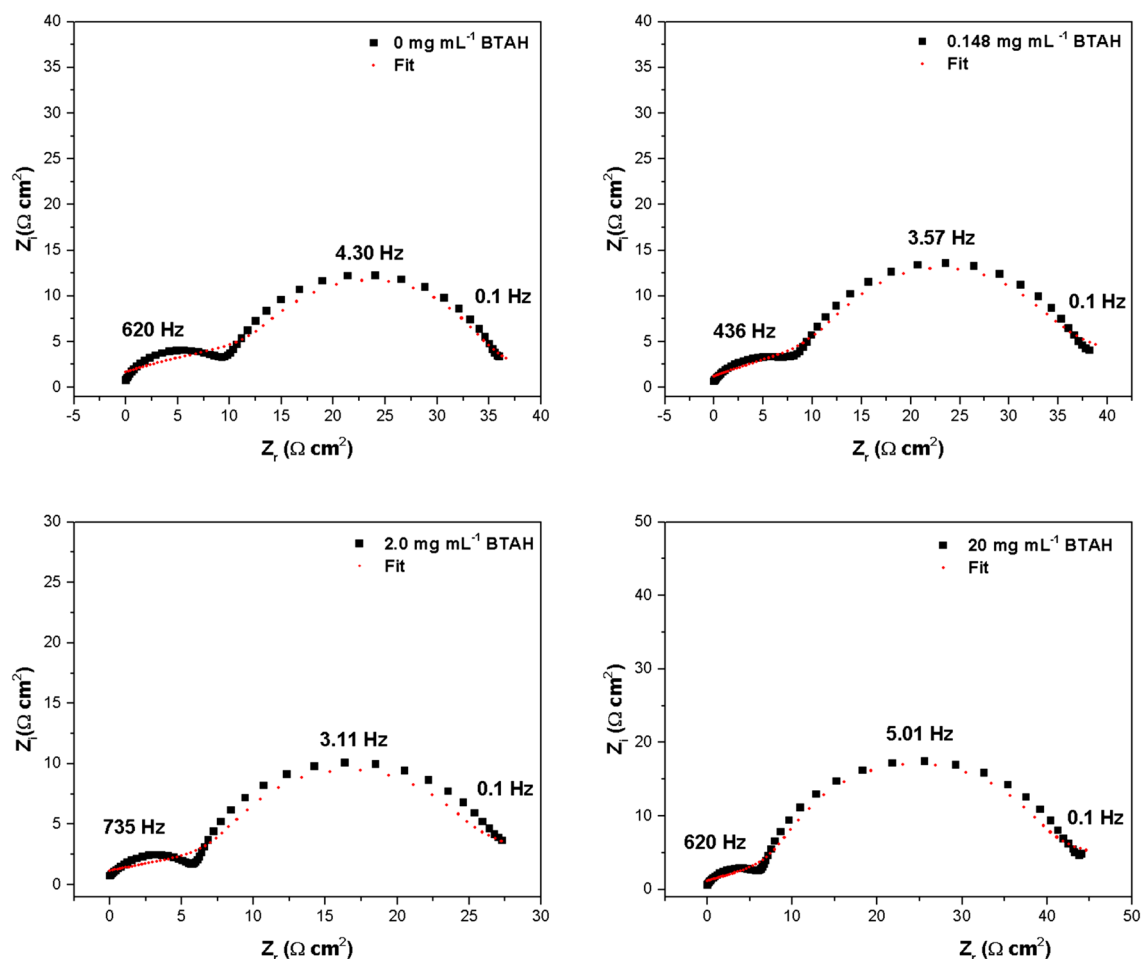
Fig.3. Nyquist plots with fitted values from DSSC with different BTAH amounts (In fitted diagrams, the Z_r was shifted to zero values to better visualization)

Table 2. - Resistances and chemical capacitance of the cells obtained by fitting the Nyquist EIS plots

BTAH (mg mL^{-1})	R_{WE} (Ω cm^2)	C_μ (mF)
0	34.2	1.57
0.148	30.2	0.98
2.0	21.8	0.72
20.0	28.6	0.36

As the IMVS operates in open circuit condition and IMPS in short circuit, it is possible to calculate the electron lifetime (τ_e) and collection lifetime (τ_c) using Eq. 2 [29, 31, 32]. The calculated results are shown in Table 3.

$$\tau = \frac{1}{2\pi f_{min}} \qquad (2)$$

In Fig. 5A, it is observed a shift to lower frequencies of the maximum frequency point to 2.0 mg mL^{-1} of BTAH

when compared to an unmodified device. This condition suggested a superior electron lifetime, which is a positive point to dye solar device and was confirmed by values in Table 2 [10, 32]. It is seen a $\tau_e = 0.041$ s and a $\tau_e = 0.034$ s to 2.0 mg mL^{-1} and 0 mg mL^{-1} of BTAH, respectively, showing a prevention of charge recombination between I_3^- with TiO$_2$ [5]. The presence of the organic structure in BTAH difficult to access of I_3^- species and these molecules also can occupy the vacancy sites in TiO$_2$ semiconductors, developing a slow back-electron recombination. On the other hand, the 20 mg mL^{-1} BTAH addition has not been presented the best η values to conditions tested, and despite superior τ_e, its present low C_μ.

In the IMPS diagram, it is also noted a shift to higher frequencies with BTAH insertion, suggesting faster collection reactions. Using Eq. 2 τ_c was calculated and an improvement in collection time was observed when BTAH was added to the dye. This behavior, evidence that the used additive has been able to boost the collection in TiO$_2$ semiconductor oxide [18]. Again, the steric effect is caused by benzene
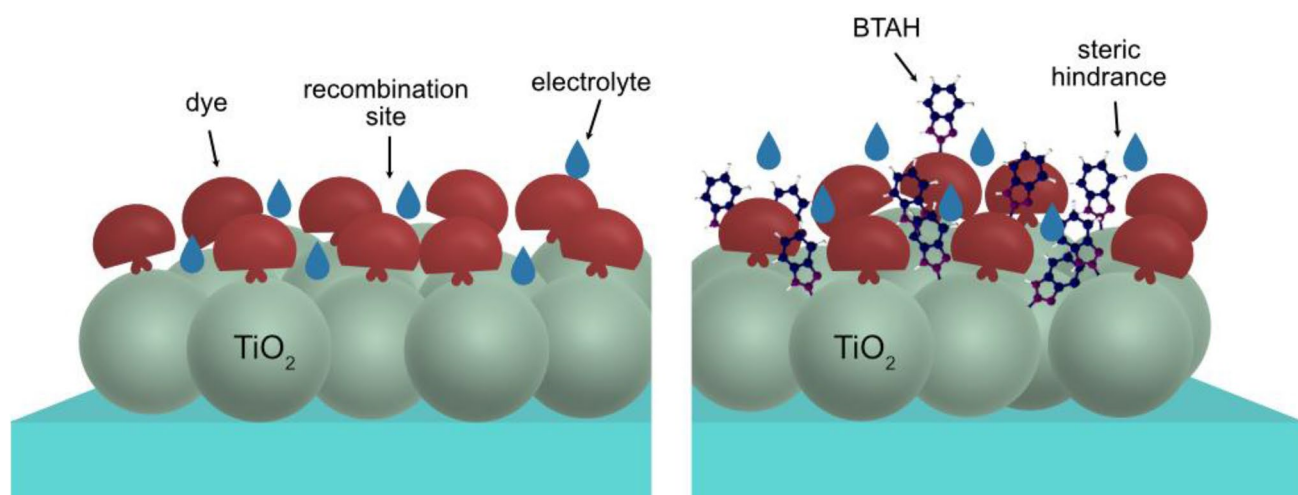
Fig. 4. Schematic overview of BTAH influence in TiO$_2$, dye/electrolyte interface
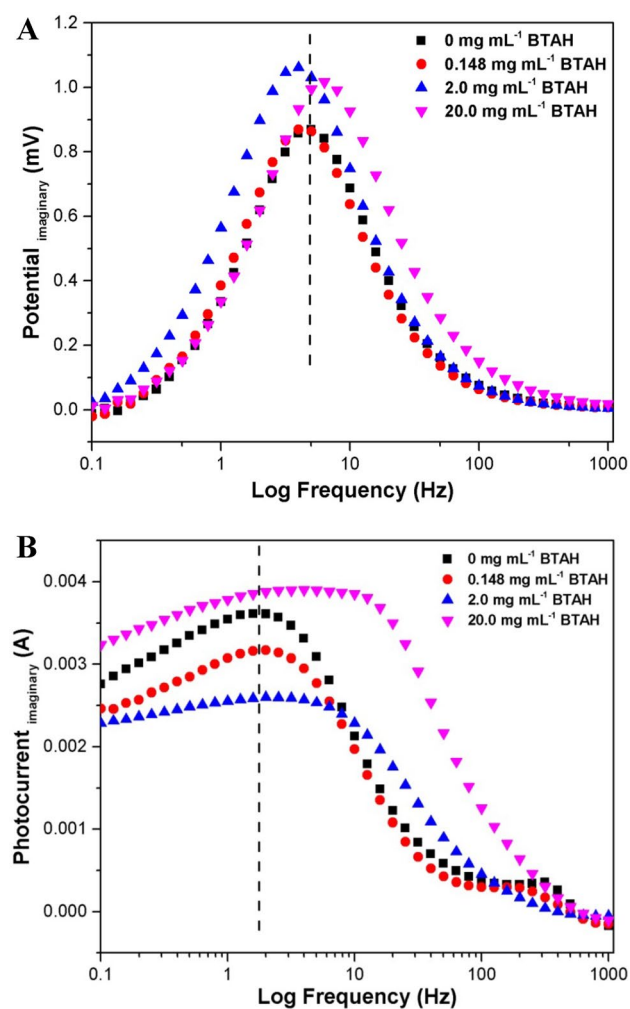

Fig. 5. a–b. IMVS diagram in 5A and IMPS in 5B to solar cells with different BTAH amounts.

Table 3. - Extracted data from the IMPS and IMVS diagrams with their respective time calculations

BTAH (mg mL^{-1})	f_{IMVS} (Hz)	τ_e (s)	f_{IMPS} (Hz)	τ_c (s)
0	4.751	0.034	1.933	0.082
0.148	4.751	0.034	2.004	0.079
2.0	3.900	0.041	3.141	0.050
20.0	6.2189	0.026	5.009	0.031

presence in a molecule, and also the N719 dye deaggregation, as the BTAH molecules might be positioning themselves between the dye molecules, rising up the charge separation and transportation in the semiconductor electrolyte interface. To 20 mg mL^{-1} of BTAH, despite amazing τ_e and τ_c presumably reduce the number of dye molecules anchored in TiO$_2$ surface, supplying less electron under solar energy incidence, supported by j_{sc} value in Table 1 [4, 11].

Then, it is important to emphasize that BTAH inserted in N719 dye solution is an amazing additive to be used in dye solar devices to enhance photoelectrochemical parameters.

Conclusions

BTAH molecules are effective additives in dye solar devices, able to enhance the photoelectrochemical parameters of the cell.

The back-electron recombination (τ_e) can be restricted and the collection time (τ_c) can be raised by BTAH presence. τ_e and τ_c enhancing are proportional to additive concentration, due to decreasing in recombination TiO$_2$/electrolyte sites. On the other hand, higher BTAH amounts,

difficult the dye anchoring, reducing the photoelectrochemical parameters.

The best solar cell was achieved at concentration of 2.0 mg mL^{-1} of BTAH, reaching a $j_{sc} = 9.92 \pm 0.26$, $V_{oc} = 0.770 \pm 0.022$, FF $= 0.557 \pm 0.014$, $\eta = 4.26 \pm 0.13$, $\tau_e = 0.034$ s and $\tau_c = 0.082$ s with lower charge transfer resistance.

References

1. Karimi-nazarabad M, Goharshadi EK, Sajjadizadeh H (2022) Copper−azolate framework coated on g - C3N4 nanosheets as a core−shell heterojunction and decorated with a Ni (OH)2 Cocatalyst for efficient photoelectrochemical water splitting. https://doi.org/10.1021/acs.jpcc.2c01570

2. M. Karimi-nazarabad, H. Ahmadzadeh, E.K. Goharshadi, Porous perovskite-lanthanum cobaltite as an efficient cocatalyst in photoelectrocatalytic water oxidation by bismuth doped g-C 3 N 4. Sol Energy **227**, 426–437 (2021). https://doi.org/10.1016/j.solener.2021.09.028

3. B. O'Regan, Grätzel M (1991) A low-cost, high-efficiency solar cell based on dye-sensitized colloidal TiO2 films. Nat **3536346**(353), 737–740 (1991). https://doi.org/10.1038/353737a0

4. A.F. Buene, D.M. Almenningen, A. Hagfeldt, O.R. Gautun, B.H. Hoff, First report of chenodeoxycholic acid-substituted dyes improving the dye monolayer quality in dye-sensitized solar cells. Sol RRL (2020). https://doi.org/10.1002/solr.201900569

5. Tractz GT, Viomar A, Dias BV, De Lima CA, Banczek EP, Da Cunha MT, Antunes SRM, Rodrigues PRP (2019) Recombination study of dye sensitized solar cells with natural extracts. J Braz Chem Soc. https://doi.org/10.21577/0103-5053.20180186

6. R. Vittal, K.C. Ho, Zinc oxide based dye-sensitized solar cells: A review. Renew Sustain Energy Rev **70**, 920–935 (2017). https://doi.org/10.1016/j.rser.2016.11.273

7. J. Lee, N. Park, Y. Shin, Solar energy materials & solar cells nano-grain SnO2 electrodes for high conversion efficiency SnO 2 – DSSC. Sol Energy Mater Sol Cells **95**, 179–183 (2011). https://doi.org/10.1016/j.solmat.2010.04.027

8. B. O'Regan, M. Grätzel, A low-cost, high-efficiency solar cell based on dye-sensitized colloidal TiO2 films. Nature **353**, 737–740 (1991). https://doi.org/10.1038/353737a0

9. Gratzel M (2001) Photoelectrochemical Cells. Nature 414:

10. T. Tractz, F. Staciaki, S. Regina, M. Antunes, P. Banczek, M. Taras, P. Rog, Nb2O5 synthesis and characterization by Pechini method to the application as electron transport material in a solar device. Sol Energy **216**, 1–6 (2021). https://doi.org/10.1016/j.solener.2021.01.029

11. D.F.S. Rodrigues, F. Santos, C.M. Abreu, J.F. Coelho, A. Serra, D. Ivanou, A. Mendes, Passivation of the TiO2 surface and promotion of N719 dye anchoring with poly(4-vinylpyridine) for efficient and stable dye- sensitized solar cells. ACS Sustain Chem Eng **9**, 5981–5990 (2021). https://doi.org/10.1021/acssuschemeng.1c00842

12. R.R. Guimaraes, A.L.A. Parussulo, T.A. Matias, H.E. Toma, K. Araki, Electrostatic blocking barrier as an effective strategy to inhibit electron recombination in DSSCs. Electrochim Acta **255**, 92–98 (2017). https://doi.org/10.1016/j.electacta.2017.09.096

13. B. Boro, B. Gogoi, B.M. Rajbongshi, A. Ramchiary, Nano-structured TiO2/ZnO nanocomposite for dye-sensitized solar cells application: a review. Renew Sustain Energy Rev **81**, 2264–2270 (2018). https://doi.org/10.1016/j.rser.2017.06.035

14. R.T. Ako, D.S.U. Peiris, P. Ekanayake, A.L. Tan, D.J. Young, Z. Zheng, V. Chellappan, DSSCs with ZnO@TiO$_2$ core-shell photoanodes showing improved Voc: Modification of energy gradients and potential barriers with Cd and Mg ion dopants. Sol Energy Mater Sol Cells **157**, 18–27 (2016). https://doi.org/10.1016/j.solmat.2016.05.009

15. G. Boschloo, L. Häggman, A. Hagfeldt, Quantification of the effect of 4-tert-butylpyridine addition to I -/I3- redox electrolytes in dye-sensitized nanostructured TiO2 solar cells. J Phys Chem B **110**, 13144–13150 (2006). https://doi.org/10.1021/jp0619641

16. P.R. Rodrigues, I. Aoki, A.H. De Andrade, E. De Oliveira, S.M. Agostinho, Effect of benzotriazole on electrochemical and corrosion behaviour of type 304 stainless steel in 2M sulphuric acid solution. Br Corros J **31**, 305–308 (2014). https://doi.org/10.1179/bcj.1996.31.4.305

17. M.T. da Cunha, P.R.P. Rodrigues, G.G.O. Cordeiro, E. D'Elia, S.M.L. Agostinho, Electrochemical studies of the interface Fe/0.5 mol L-1 H2SO4 in the presence of benzotriazole and tolytriazole. Mater Chem Phys **116**, 469–473 (2009). https://doi.org/10.1016/j.matchemphys.2009.04.025

18. T. Valerio, G.T. Tractz, G.A.R. Maia, E.P. Banczek, P.R.P. Rodrigues, Minimizing of charge recombination by Nb 2 O 5 addition in dye-sensitized solar cells. Opt Mater (2020). https://doi.org/10.1016/j.optmat.2020.110310

19. E.P. Banczek, P.R.P. Rodrigues, I. Costa, Investigation on the effect of benzotriazole on the phosphating of carbon steel. Surf Coat Technol **201**, 3701–3708 (2006). https://doi.org/10.1016/j.surfcoat.2006.09.003

20. M.M. Mennucci, E.P. Banczek, P.R.P. Rodrigues, I. Costa, Evaluation of benzotriazole as corrosion inhibitor for carbon steel in simulated pore solution. Cem Concr Compos **31**, 418–424 (2009). https://doi.org/10.1016/j.cemconcomp.2009.04.005

21. A. Viomar, G.A.R. Maia, F.R. Scremin, N.M. Khalil, M.T. Cunha, A.C. Antunes, P.R.P. Rodrigues, Influence of obtaining method of Nb2O5 particles used in dye sensitized solar cells consisting of TiO $_2$ / Nb $_2$ O $_5$. Rev Virtual Química (2016). https://doi.org/10.5935/1984-6835.20160064

22. A. Gopalaraman, S. Karuppuchamy, S. Vijayaraghavan, High efficiency dye-sensitized solar cells with: V OC- J SC trade off eradication by interfacial engineering of the photoanode|electrolyte interface. RSC Adv **9**, 40292–40300 (2019). https://doi.org/10.1039/c9ra08278f

23. S. Kundu, P. Sarojinijeeva, R. Karthick, G. Anantharaj, G. Saritha, R. Bera, S. Anandan, A. Patra, P. Ragupathy, M. Selvaraj, D. Jeyakumar, K.V. Pillai, Enhancing the efficiency of DSSCs by the modification of TiO2 photoanodes using N, F and S, co-doped graphene quantum dots. Electrochim Acta **242**, 337–343 (2017). https://doi.org/10.1016/j.electacta.2017.05.024

24. G.G. Sonai, A. Tiihonen, K. Miettunen, P.D. Lund, A.F. Nogueira, Long-term stability of dye-sensitized solar cells assembled with cobalt polymer gel electrolyte. J Phys Chem C **121**, 17577–17585 (2017). https://doi.org/10.1021/acs.jpcc.7b03865

25. Tractz T, Paula A, Matheus C, Fernanda L, Larsson G, Rodrigues P (2022) The use of 2-Mercaptobenzothiazole as a new co-adsorbent in dye-sensitized solar cells. 131: . https://doi.org/10.1016/j.optmat.2022.112658

26. K. Ocakoglu, F. Yakuphanoglu, J.R. Durrant, S. Icli, The effect of temperature on the charge transport and transient absorption

properties of K27 sensitized DSSC. Sol Energy Mater Sol Cells **92**, 1047–1053 (2008). https://doi.org/10.1016/j.solmat.2008.03.006

27. S. Kushwaha, S. Mandal, S. Subramanian, S. Aryasomayajul, K. Ramanujam, A DSSC with an efficiency of ~10 %: fermi level manipulation impacting the electron transport at the photoelectrode-electrolyte interface. ChemistrySelect **1**, 6179–6187 (2016). https://doi.org/10.1002/slct.201601461

28. C. Longo, M.A. De Paoli, Dye-sensitized solar cells: a successful combination of materials. J Braz Chem Soc **14**, 889–901 (2003). https://doi.org/10.1590/S0103-50532003000600005

29. J. Bisquert, V.S. Vikhrenko, Interpretation of the time constants measured by kinetic techniques in nanostructured semiconductor electrodes and dye-sensitized solar cells. J Phys Chem B **108**, 2313–2322 (2004). https://doi.org/10.1021/jp035395y

30. Hagfeldt A, Boschloo G, Sun L, Kloo L, Pettersson H (2010) 2010 ChemReview_Hagfeldt.pdf. 6595–6663

31. P. Xiang, F. Lv, T. Xiao, L. Jiang, X. Tan, T. Shu, Improved performance of quasi-solid-state dye-sensitized solar cells based on iodine-doped TiO2 spheres photoanodes. J Alloys Compd **741**, 1142–1147 (2018). https://doi.org/10.1016/j.jallcom.2018.01.220

32. L.L. Li, Y.C. Chang, H.P. Wu, E.W.G. Diau, Characterisation of electron transport and charge recombination using temporally resolved and frequency-domain techniques for dye-sensitised solar cellse. Int Rev Phys Chem **31**, 420–467 (2012). https://doi.org/10.1080/0144235X.2012.733539